Optimized Effective Potential Model for the Double Perovskites $Sr_{2-x}Y_xVMoO_6$ and $Sr_{2-x}Y_xVTcO_6$

I V Solovyev

National Institute for Materials Science, 1-2-1 Sengen, Tsukuba, Ibaraki 305-0047, Japan

E-mail: solovyev.igor@nims.go.jp

Abstract. In attempt to explore half-metallic properties of the double perovskites $Sr_{2-x}Y_xVMoO_6$ and $Sr_{2-x}Y_xVTcO_6$, we construct an effective low-energy model, which describes the behavior of the t_{2q} -states of these compounds. All parameters of such model are derived rigorously on the basis of first-principles electronic structure calculations. In order to solve this model we employ the optimized effective potential method and treat the correlation interactions in the random phase approximation. Although correlation interactions considerably reduce the intraatomic exchange splitting in comparison with the Hartree-Fock method, this splitting still substantially exceeds the typical values obtained in the local-spin-density approximation (LSDA), which alters many predictions based on the LSDA. Our main results are summarized as follows: (i) all ferromagnetic states are expected to be half-metallic. However, their energies are generally higher than those of the ferrimagnetic ordering between V- and Mo/Tc-sites (except Sr₂VMoO₆); (ii) all ferrimagnetic states are metallic (except fully insulating Y₂VTcO₆) and no half-metallic antiferromagnetism has been found; (iii) moreover, many of the ferrimagnetic structures appear to be unstable with respect to the spin-spiral alignment. Thus, the true magnetic ground state of the most of these systems is expected to be more complex. In addition, we discuss several methodological issues related to the nonuniqueness of the effective potential for the magnetic halfmetallic and insulating states.

PACS numbers: 75.25.-j, 72.80.Ga, 71.10.-w, 75.47.-m

1. Introduction

Recently double perovskites $A_{2-x}A'_xBB'O_6$, where A and A' are the di- and three-valent (typically alkali-earth or rare-earth) elements, respectively, and B (B') are the transition-metal elements, have attracted considerable attention [1], following experimental discoveries of the room-temperature ferromagnetism and the colossal-magnetoresistance effect in Sr_2FeMoO_6 [2], which make these materials promising in the field of spin electronics. The extraordinary properties of the double perovskites are frequently attributed to their half-metallic electronic structure, although the situation can be rather subtle [3]. Nevertheless, the first discoveries spark the new research activity aiming at the systematic search of half-metallic double-perovskite materials. Many such predictions has been made on the basis of first-principles electronic structure calculations. Besides ferromagnetic (FM) compounds, a particular attention was paid to the half-metallic antiferromagnets – the systems, where the half-metallicity coexists with the zero net magnetization [4, 5]. However, even apart from the technological issues, related to the defects in the double-perovskite structure, there is a number of fundamental problems, which call many predictions into question:

- (i) Most of the calculations are based on the local-spin-density approximation (LSDA) or its refinement the generalized gradient approximation, which have many limitations for the transition-metal oxides. Particularly, all these theories employ the functional dependence of the exchange-correlation energy obtained in the limit of homogeneous electron gas. However, many unique properties of the double perovskites are related to the alternation of two different transition-metal sites B and B', and in this sense the systems are essentially inhomogeneous. Thus, even though the double-perovskite compounds may be classified as itinerant electron magnets, it does not necessary mean that their properties are well described within LSDA;
- (ii) In the vast majority of calculations, it is believed that the LSDA+U technique, which incorporates the physics of on-site Coulomb interactions [6, 7], can serve as a reasonable alternative to LSDA and provide more superior description for the properties of double perovskites. However, the LSDA+U scheme for the double perovskites is ill-defined: there are many uncertainties related to the values of the on-site Coulomb repulsion U at the sites B and B', which are frequently taken as adjustable parameters, the subspace of "localized orbitals", and the double-counting term [8]. Moreover, the total energy in LSDA+U is taken in the ad hoc form, which is valid only in the atomic limit and equivalent to some constrained density-functional theory [7]. In such a situation, all predictions of the half-metallic behavior for the double perovskites should be taken very cautiously.

In this paper we will illustrate how these problem could be resolved by applying the optimized effective potential (OEP) method, and what the consequences on the electronic and magnetic properties of the double perovskites could be. The OEP method is formulated in the spirit of Kohn-Sham density functional theory [9], by introducing an auxiliary one-electron problem, which is specified by some local effective potential and which is used for the search of the true spin density through the minimization of the total energy of the system [10, 11, 12, 13]. In this work we will apply the OEP technique for the solution of the low-energy model, where all the parameters are derived rigorously, on the basis of first-principles electronic structure calculations. Besides simplicity, such a model analysis typically allows one to concentrate directly on the microscopic picture, underlying the considered phenomena. For the first applications of the OEP model, it is more convenient to consider the t_{2g} -systems, whose electronic and magnetic properties are predetermined by the behavior of the t_{2g} -states of the sites B and B' located near the Fermi level. In this case, the effective potential is specified by only three parameters, which should be used for the minimization of the total energy.

We select two prototypical examples $Sr_{2-x}Y_xVMoO_6$ and $Sr_{2-x}Y_xVTcO_6$, for which we adopt the undistorted double perovskite structure with the lattice parameters a=7.846 and 7.899 Å, respectively. In fact, a=7.846 Å is the experimental lattice constant for $SrLaVMoO_6$ [14], which is close to theoretical values obtained in the first-principles calculations [15], and a=7.899 Å is the theoretical lattice constant for La_2VTcO_6 [16]. Deviations from the ideal double perovskite structure are expected to be small [16] and were not considered here. The band-filling dependence due to the substitution of Sr by Y was treated in the virtual-crystal approximation. According to the electronic structure calculations in the local-density approximation (LDA), the basic difference between Sr_2VMoO_6 and Sr_2VTcO_6 is in the relative position of the V- and Mo(Tc)-states: in Sr_2VMoO_6 , the V- and a state of V- and V- and a state of V- and V- and a state of V- and V- and V- and V- and a state of V- and V- and V- and V- and a state of V- and a state of V- and V- and V- and V- and V- and a state of V- and V- and a state of V- and V- and a state of V- and a

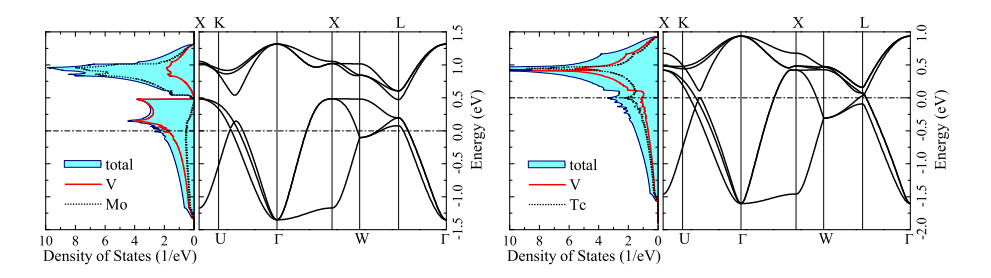


Figure 1. Electronic structure near the Fermi level in the local-density approximation (total and partial densities of states, and the energy dispersion of the t_{2g} -bands) for Sr_2VMoO_6 (left) and Sr_2VTcO_6 (right). The position of the Fermi level is shown by the dot-dashed line.

compounds compounds) were intensively discussed in the literature in the context of the half-metallic applications. For instance, SrLaVRuO₆, SrLaVMoO₆, and La₂VTcO₆ were proposed to be the half-metallic antiferromagnets [14, 16, 17, 18]. On the other hand, the metallic ferrimagnetic (i.e., non spin-compensated) behavior was also suggested for SrLaVMoO₆ [15, 19]. In general, such conclusions are sensitive to the values of the

on-site Coulomb repulsion U, which are used in the calculations.

The rest of the paper is organized as follows. The method is discussed in Sec. 2. Particularly, in Sec. 2.1 we briefly describe construction of the low-energy model for the double perovskites and in Sec. 2.2 – the basic idea of the OEP method. Results of the model OEP calculations are shown in Sec. 3. Particularly, the obtained electronic band structure is discussed in Sec. 3.1, the screening of on-site interactions due to the correlation effects and its consequences on the properties of $Sr_{2-x}Y_xVMoO_6$ and $Sr_{2-x}Y_xVTcO_6$ is considered in Sec. 3.2, and the behavior of the total energy and stability of the ferrimagnetic states are discussed in Sec. 3.3. Finally, brief summary of the work is presented in Sec. 4.

2. Method

2.1. Construction and parameters of the low-energy model

The first step of our approach is the construction of the effective low-energy model for the t_{2q} -states of the double perovskites:

$$\hat{\mathcal{H}} = \sum_{ij} \sum_{\sigma} \sum_{mm'} t_{ij}^{mm'} \hat{c}_{im\sigma}^{\dagger} \hat{c}_{jm'\sigma} + \frac{1}{2} \sum_{i} \sum_{\sigma\sigma'} \sum_{mm'm''m'''} U_{mm'm''m'''}^{i} \hat{c}_{im\sigma}^{\dagger} \hat{c}_{im''\sigma}^{\dagger} \hat{c}_{im''\sigma'}^{\dagger} \hat{c}_{im''\sigma'}, \quad (1)$$

which is derived in the Wannier basis, by starting from the LDA band structure. The Wannier functions are specified by the indices m = xy, yz, or zx, and σ stands for the spin indices \uparrow or \downarrow . The one-electron part $t_{ij}^{mm'}$ of the model Hamiltonian was derived by using downfolding method, and the Coulomb (and exchange) interactions $U_{mm'm''m''}^{i}$ were obtained by combining the constrained density-functional theory with the random-phase approximation (RPA). The method was discussed in the literature, and for details the reader is referred to the review article [20]. There are three sets of parameters in the model Hamiltonian (1):

- (i) the "charge transfer" energies, or the energy splitting between "atomic" t_{2g} -levels of the V and Mo (Tc) sites, which are described by the site-diagonal part of $t_{ij}^{mm'}$. The values of these parameters are -391 and 94 meV for the VMo and VTc compounds, respectively. Thus, as expected from the LDA band structure (Fig. 1), for the VMo compounds, the atomic V-states are located lower in energy and well separated from the Mo-states, while for the VTc compounds, the situation is reversal and the splitting is considerably smaller;
- (ii) the transfer integrals, which are described by the off-diagonal elements of $t_{ij}^{mm'}$ with respect to the site indices. As expected, the largest parameter is the $dd\pi$ -transfer integral between nearest-neighbor V- and Mo(Tc)-sites, which is 271 (245) meV. Another important parameter is the $dd\sigma$ -transfer integral between next nearest neighbors of the same atomic type. Its values in the V- and Mo-sublattices of the VMo compounds are -72 and -116 meV, respectively. Similar values were obtained for the VTc compounds: -73 and -113 meV for the V- and Tc-sublattice, respectively;

(iii) intraatomic Coulomb and exchange interactions in the t_{2g} -band, which are screened by all other states. At each site of the system, these interactions are fully specified by two Kanamori parameters [21]: the intraorbital Coulomb interaction $\mathcal{U} = U_{mmmm}$ and the exchange interaction $\mathcal{J} = U_{mm'm'm}$ for $m \neq m'$. In the perfect cubic environment, the third Kanamori parameter $\mathcal{U}' = U_{mmm'm'}$ (the interorbital Coulomb interaction) can be related to \mathcal{U} and \mathcal{J} as $\mathcal{U}' = \mathcal{U} - 2\mathcal{J}$ [20]. Other types of matrix elements of $||U_{mm'm''m'''}||$ are equal to zero. The band-filling dependence of \mathcal{U} , \mathcal{U}' , and \mathcal{J} , as obtained in the virtual crystal approximation, is explained in Fig. 2. Generally, as the number of t_{2g} -electrons increases, the effective Coulomb

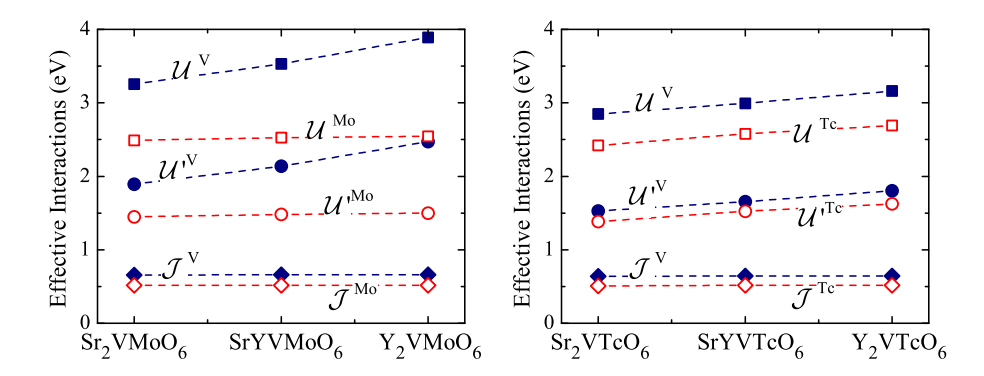


Figure 2. Intraorbital Coulomb interaction \mathcal{U} , interorbital Coulomb interaction \mathcal{U}' , and the exchange interaction \mathcal{J} for the $\mathrm{Sr}_{2-x}\mathrm{Y}_x\mathrm{VMoO}_6$ (left) and $\mathrm{Sr}_{2-x}\mathrm{Y}_x\mathrm{VTcO}_6$ (right) compounds.

interactions also increase, reflecting the tendencies of the RPA screening [20]. On the other hand, the effective exchange interaction \mathcal{J} is less sensitive to the band filling. The Coulomb repulsion \mathcal{U}^{V} is larger for the VMo-compounds, due to the specific electronic structure of $\operatorname{Sr}_{2-x}\operatorname{Y}_{x}\operatorname{VMoO}_{6}$ (Fig. 1): since the V-band is separated and located in the low-energy part of the spectrum, it will be populated in the process of the band-filling. It will effectively reduce the number of channel available for the RPA screening of \mathcal{U}^{V} , for example, due to the transitions from the occupied oxygen band to the unoccupied part of the V-band [20]. Thus, \mathcal{U}^{V} will be less screened in the VMo-systems in comparison with the VTc-ones, where the V-and Tc-states form one common band (Fig. 1).

2.2. Optimized effective potential method

In order to solve the model and find the magnetic ground state of the double perovskites, we employ the optimized effective potential method. The OEP model works in the spirit of the Kohn-Sham density functional theory [9] on the double-perovskite lattice, where the kinetic energy

$$E_{\rm kin} = \sum_{\sigma} \sum_{n}^{\rm occ} \frac{1}{\Omega_{\rm BZ}} \int d\mathbf{k} \langle c_{\sigma n \mathbf{k}} | \hat{t}_{\mathbf{k}} | c_{\sigma n \mathbf{k}} \rangle,$$

the number of electrons

$$n^{\tau} = \sum_{\sigma} \sum_{m} \sum_{n}^{\text{occ}} \frac{1}{\Omega_{\text{BZ}}} \int d\mathbf{k} c_{\sigma n \mathbf{k}}^{m \tau \dagger} c_{\sigma n \mathbf{k}}^{m \tau},$$

and the spin magnetic moment

$$m^{\tau} = \sum_{m} \sum_{n}^{\text{occ}} \frac{1}{\Omega_{\text{BZ}}} \int d\mathbf{k} \left(c_{\uparrow n\mathbf{k}}^{m\tau\dagger} c_{\uparrow n\mathbf{k}}^{m\tau} - c_{\downarrow n\mathbf{k}}^{m\tau\dagger} c_{\downarrow n\mathbf{k}}^{m\tau} \right)$$

at the site τ are constructed from the one-electron orbitals $c_{\sigma n\mathbf{k}}$, which are obtained from the solution of the auxiliary one-electron problem

$$\left(\hat{t}_{\mathbf{k}} + \hat{v}_{\text{eff}}^{\sigma}\right) |c_{\sigma n \mathbf{k}}\rangle = \varepsilon_{\sigma n \mathbf{k}} |c_{\sigma n \mathbf{k}}\rangle \tag{2}$$

with the potential $\hat{v}_{\text{eff}}^{\sigma}$. In the above notations, $\hat{t}_{\mathbf{k}}$ is the Fourier image of $\hat{t}_{ij} = ||t_{ij}^{mm'}||$, each eigenvector $|c_{\sigma n\mathbf{k}}\rangle$ is specified by its components $c_{\sigma n\mathbf{k}}^{m\tau}$ in the basis of t_{2g} -orbitals m = xy, yz, or zx of the atomic type $\tau = V$ or Mo(Tc), n is the band index, and \mathbf{k} is the position in the first Brillouin zone with the volume Ω_{BZ} .

The parameters of the potential $\hat{v}_{\text{eff}}^{\sigma}$, which is supposed to be "local" (or diagonal with respect to the site indices), are obtained from the minimization of the total energy

$$E = E_{\rm kin} + E_{\rm C} + E_{\rm X} + E_{\rm corr},\tag{3}$$

where the Coulomb $(E_{\rm C})$ and exchange $(E_{\rm X})$ energies are given by

$$E_{\rm C} = \frac{1}{2} \sum_{\tau} \sum_{\sigma \sigma'} \sum_{mm'm''m'''} U_{mm'm''m'''}^{\tau} n_{mm'}^{\sigma\tau} n_{m''m'''}^{\sigma'\tau}$$

and

$$E_{\rm X} = -\frac{1}{2} \sum_{\tau} \sum_{\sigma} \sum_{mm'm''m'''} U^{\tau}_{mm'''m'''n} n^{\sigma\tau}_{mm'} n^{\sigma\tau}_{m''m'''},$$

respectively, in terms of the density matrix:

$$n_{mm'}^{\sigma\tau} = \sum_{n=1}^{\text{occ}} \frac{1}{\Omega_{\text{BZ}}} \int d\mathbf{k} c_{\sigma n \mathbf{k}}^{m\tau\dagger} c_{\sigma n \mathbf{k}}^{m'\tau}.$$

The expression for the correlation energy, which is treated in the random phase approximation, is given by [22, 23, 24]:

$$E_{\text{corr}} = -\frac{1}{4\Omega_{\text{BZ}}} \int d\mathbf{q} \text{Tr} \left\{ \ln \left[1 - \hat{P}(i\omega, \mathbf{q}) \hat{U} \right] \left[1 - \hat{U} \hat{P}(i\omega, \mathbf{q}) \right] + 2\hat{P}(i\omega, \mathbf{q}) \hat{U} \right\}, \tag{4}$$

where \hat{U} are the diagonal matrices $\|U^{\tau}_{mm'm''m'''}\|$ with respect to the site indices τ , $\hat{P} = \|P^{\tau\tau'}_{mm'm''m'''}\|$ is the polarization in the imaginary frequency:

$$P_{mm'm''m'''}^{\tau\tau'}(i\omega,\mathbf{q}) = \sum_{\sigma} \sum_{n}^{\text{occ}} \sum_{n'}^{\text{unocc}} \frac{1}{\Omega_{\text{BZ}}} \int d\mathbf{k} \frac{2(\varepsilon_{\sigma n\mathbf{k}} - \varepsilon_{\sigma n'\mathbf{k}+\mathbf{q}})}{\omega^2 + (\varepsilon_{\sigma n\mathbf{k}} - \varepsilon_{\sigma n'\mathbf{k}+\mathbf{q}})^2} c_{\sigma n'\mathbf{k}+\mathbf{q}}^{m\tau\dagger} c_{\sigma n\mathbf{k}}^{m'\tau} c_{\sigma n'\mathbf{k}+\mathbf{q}}^{m''\tau'} c_{\sigma n'\mathbf{k}+\mathbf{q}}^{m''\tau'}, (5)$$

and matrix multiplication in (4) implies the convolution over two orbital indices: $(\hat{U}\hat{P})_{mm'm''m'''}^{\tau\tau'} = \sum_{ll'} U_{mm'll'}^{\tau} P_{ll'm''m'''}^{\tau\tau'}$.

For the cubic systems (and neglecting the orbital polarization effects), the effective potential is specified by three parameters: $\hat{v}_{\rm eff}^{\uparrow V} = -\Delta_{\rm ex}^{\rm V}/2$, $\hat{v}_{\rm eff}^{\downarrow V} = \Delta_{\rm ex}^{\rm V}/2$, $\hat{v}_{\rm eff}^{\rm Mo(Tc)} = \Delta_{\rm ct} - \Delta_{\rm ex}^{\rm Mo(Tc)}/2$, and $\hat{v}_{\rm eff}^{\rm Mo(Tc)} = \Delta_{\rm ct} + \Delta_{\rm ex}^{\rm Mo(Tc)}/2$. In the other words, $\Delta_{\rm ex}^{\rm V}$ and $\Delta_{\rm ex}^{\rm Mo(Tc)}$ is the exchange-correlation splitting between minority- and majority-spin states at the sites V and Mo(Tc), respectively, and $\Delta_{\rm ct}$ is the "charge transfer energy" between sites V and Mo(Tc). All these parameters are obtained by minimizing the total energy (3). In practice, first we calculate the total energy on some coarse mesh of these parameters, identify the minimum, then continue the calculations around the minimum by using finer mesh, and so on until reaching necessary accuracy for the total energy minimum (less than 1 meV).

3. Results and Discussions

3.1. Electronic structure and arbitrariness of the OEP procedure for half-metallic and insulating states

In the following, we consider two magnetic solutions: ferromagnetic $(\Delta_{\rm ex}^{\rm V}>0$ and $\Delta_{\rm ex}^{\rm Mo(Tc)}>0)$ and ferrimagnetic $(\Delta_{\rm ex}^{\rm V}>0$, while $\Delta_{\rm ex}^{\rm Mo(Tc)}<0)$, and find parameters of the effective potential by minimizing the total energy for each case. Total and partial densities of states for ${\rm Sr}_{2-x}{\rm Y}_x{\rm VMoO}_6$, obtained from the solution of the Kohn-Sham equations (2) with the optimized potential, are shown in Fig. 3. All FM solutions are

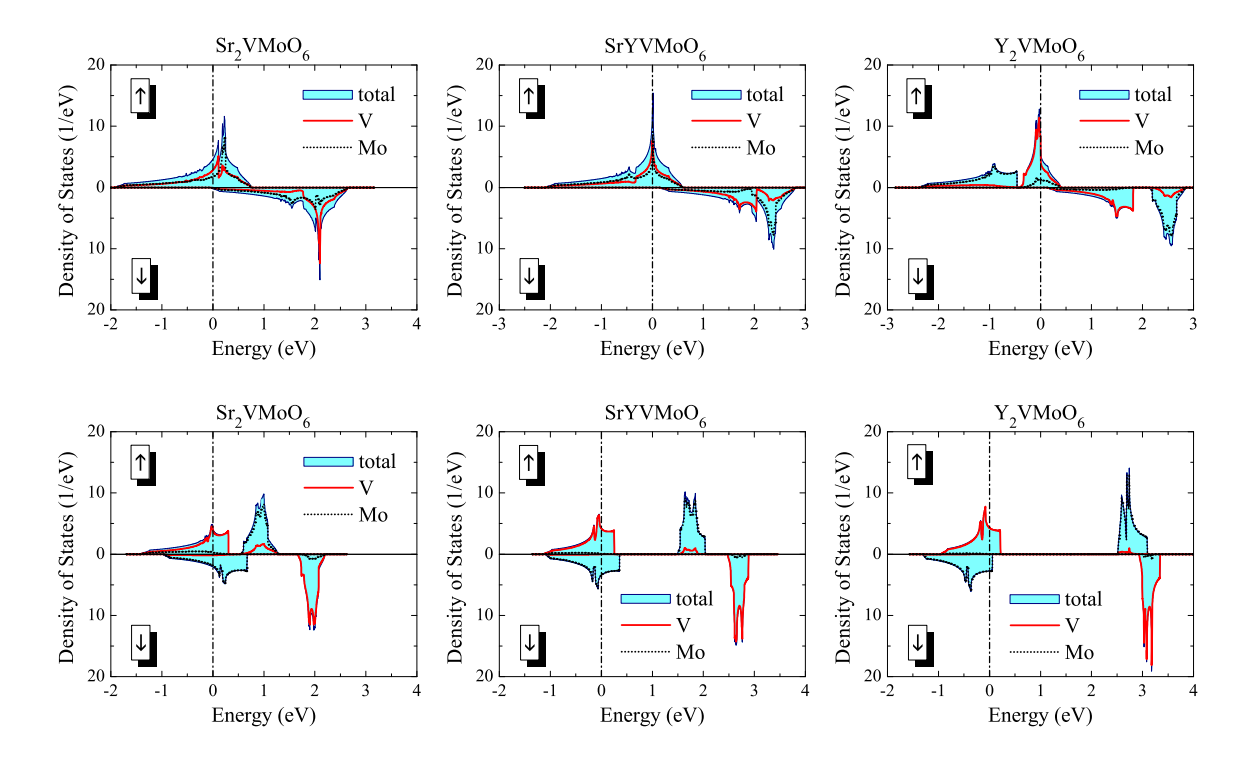


Figure 3. Total and partial densities of states as obtained in the optimized effective potential method for the ferromagnetic (upper panel) and ferrimagnetic (lower panel) configurations of $Sr_{2-x}Y_xVMoO_6$. The Fermi level is at zero energy.

half-metallic: the Fermi levels crosses the majority-spin band, while the minority-spin band is completely empty. In the case of Sr_2VMoO_6 and $SrYVMoO_6$, there is a strong hybridization between V- and Mo-states, which form the common majority-spin band. However, in Y_2VMoO_6 the majority-spin band is split into the Mo- and V-subbands, which are separated by an energy gap. This behavior is related to the large Coulomb repulsion \mathcal{U}^V in Y_2VMoO_6 (Fig. 2), which additionally shifts the V-states to the higher-energy part of spectrum. Any deviation from the half-metallic behavior and partial population of the minority-spin band increases the total energy of $Sr_{2-x}Y_xVMoO_6$ and thus makes this state unstable.

The choice of the parameters of the effective potential in the half-metallic regime is not unique. For example, any redistribution of states in the unoccupied minority-spin band does not affect the ground-state properties. Moreover, any change of $\Delta_{\rm ex}^{\rm V}$, $\Delta_{\rm ex}^{\rm Mo}$, and $\Delta_{\rm ct}$, which does not deform the partially populated majority-spin band (apart from the constant shift), does not affect the ground-state properties either. Quantitatively, this condition can be formulated as follows: the ground-state properties in the half-metallic regime are controlled by the single parameter $a = \Delta_{\rm ct} + (\Delta_{\rm ex}^{\rm V} - \Delta_{\rm ex}^{\rm Mo})/2$. Any change of $\Delta_{\rm ex}^{\rm V}$, $\Delta_{\rm ex}^{\rm Mo}$, and $\Delta_{\rm ct}$, which keeps a, does not affect the ground-state properties in the half-metallic regime.

All ferrimagnetic configurations of $Sr_{2-x}Y_xVMoO_6$ are metallic. In this case all three parameters of the effective potential are uniquely defined. The degree of the spin polarization (P) in the ferrimagnetic state is sensitive to the concentration x and the definition of P [25]. For example, using the simplest "density of states" definition (see Fig. 3), one obtains P=0.3, 0.1, and 0.2 for x=0, 1 and 2, respectively. On the other hand, the "Bloch-Bolzmann transport theory" definition yields P=0.1, 0.1, and 0.5 for x=0, 1 and 2, respectively. The experimental value of P for SrLaVMoO₆, measured by using the point-contact Andreev reflection technique, is about 0.5 [14]. Nevertheless, as we will see below, many of these ferrimagnetic states appear to be unstable and calculated spin polarization cannot be directly compared with the experimental data.

Similar behavior was obtained for Sr₂VTcO₆ and SrYVTcO₆, where again half-metallic FM state competes with the normal metallic ferrimagnetic state (Fig. 4)

 Y_2VTcO_6 requires a special attention: it has six electrons in the t_{2g} -band. The system is insulating and all metallic configurations have higher energies. Therefore, in the FM state, the parameters $\Delta_{\rm ex}^{\rm V}$, $\Delta_{\rm ex}^{\rm Tc}$, and $\Delta_{\rm ct}$ can be chosen in an arbitrary way. Indeed, any combination of these parameters (provided that the system remains insulating) yields the same number of electrons $n^{\tau}=3$, spin magnetic moments $m^{\tau}=3\mu_B$, and the total energy of the system. The correlation energy is exactly equal to zero for this particular case. The arbitrariness with the choice of the effective potential remains also in the antiferromagnetic state of Y_2VTcO_6 (Fig. 5), although the number of arbitrary parameters decreases. Indeed, the splitting between V- and Mo-states with the same spin affects the ground-state properties. However, the bands with different spins can be rigidly shifted relative to each other and, as long as the system remains in the insulating state, this shift does not affect the ground-state properties. Thus,

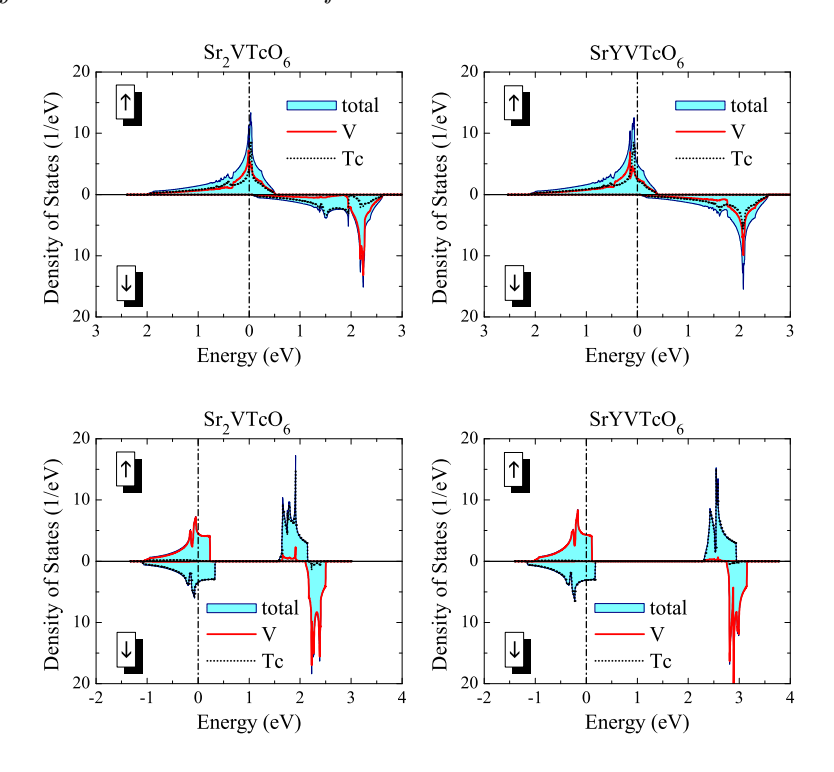


Figure 4. Total and partial densities of states as obtained in the optimized effective potential method for the ferromagnetic (upper panel) and ferrimagnetic (lower panel) configurations of Sr₂VTcO₆ and SrYVTcO₆. The Fermi level is at zero energy.

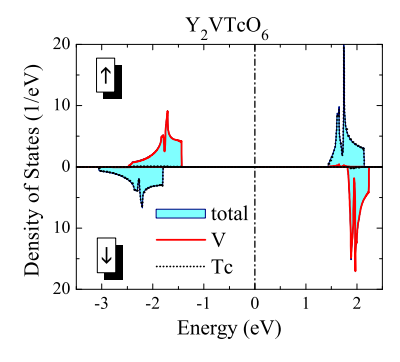


Figure 5. Total and partial densities of states as obtained in the optimized effective potential method for the antiferromagnetic configuration of Y_2VTcO_6 . The Fermi level lies in the band gap.

the properties of the antiferromagnetic Y_2VTcO_6 are defined by only two parameters: $\Delta_{\rm ct}$ and $(\Delta_{\rm ex}^{\rm V} - \Delta_{\rm ex}^{\rm Tc})$, while the third parameter $(\Delta_{\rm ex}^{\rm V} + \Delta_{\rm ex}^{\rm Tc})$ can be taken arbitrarily. Finally, we would like to emphasize that antiferromagnetic Y_2VTcO_6 becomes insulating due to the large exchange splitting (both at the V- and Tc-sites) obtained in the OEP calculations. If the splitting were smaller, the majority-spin V- and Tc-bands would eventually merge, yielding the half-metallic antiferromagnetic state, which was obtained in the LSDA calculations for the isoelectronic La₂VTcO₆ [16]. Thus, such half-metallic

antiferromagnetic state is probably an artifact of LSDA, and more rigorous treatment of the correlation effects will open the band gap in the both spin channels.

3.2. Screening and the effective Stoner model

Since the effective potential is local (or diagonal with respect to the site indices) and does not affect the orbital degrees of freedom, the OEP scheme has many similarities with the Stoner model of magnetism, where the strength of the intraatomic splitting $\Delta_{\text{ex}}^{\tau}$ between the minority- and majority-spin states is controlled by the effective parameter I^{τ} : $\Delta_{\text{ex}}^{\tau} = I^{\tau}m^{\tau}$. Thus, using the intraatomic exchange splitting, obtained from the minimization of the total energy, and corresponding values of the spin magnetic moments in the ground state (Fig. 6), one can find the effective Stoner parameter I_{OEP}^{τ} . All such

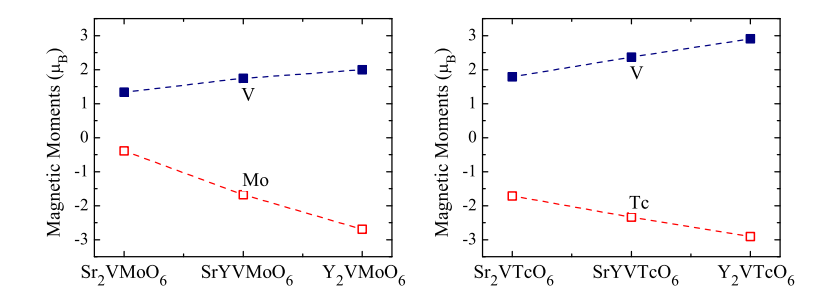


Figure 6. Local spin magnetic moments at the V- and Mo(Tc)-sites, as obtained in the optimized effective potential method for $Sr_{2-x}Y_xVMoO_6$ (left) and $Sr_{2-x}Y_xVTcO_6$ (right).

considerations are valid only for the ferrimagnetic metallic state, where $\Delta_{\rm ex}^{\tau}$ are uniquely defined. The results for ${\rm Sr}_{2-x}{\rm Y}_x{\rm VMoO_6}$ are explained in Fig. 7. The effective Stoner parameters derived from the OEP approach are of the order of 1.3-1.6 eV at the V-sites and 1.0-1.1 eV at the Mo-sites. Similar parameters were obtained for ${\rm Sr}_{2-x}{\rm Y}_x{\rm VTcO_6}$: $I_{\rm OEP}^{\rm V}=1.27$ eV and $I_{\rm OEP}^{\rm Tc}=1.06$ eV in the case of ${\rm Sr}_2{\rm VTcO_6}$, and $I_{\rm OEP}^{\rm V}=1.28$ eV and $I_{\rm OEP}^{\rm Tc}=1.18$ eV in the case of ${\rm Sr}_2{\rm VTcO_6}$. All of them are systematically larger that the typical values of I^{τ} obtained in the local-spin-density approximation (typically, close 1 eV for the 3*d*-elements and even smaller for the 4*d*- and 5*d*-elements [26]). This example clearly shows the importance of the rigorous treatment of the exchange-correlation interactions (beyond LSDA) in the physics of double perovskites.

Another limiting case is the Hartree-Fock (HF) approximation, which neglects the correlation interactions. Then, corresponding Stoner parameter describing the splitting in the system of three t_{2g} -orbitals, are given by $I_{\rm HF}^{\tau} = (\mathcal{U}^{\tau} + 2\mathcal{J}^{\tau})/3$. They are also plotted in Fig. 7. The difference between $I_{\rm HF}^{\tau}$ and $I_{\rm OEP}^{\tau}$ is the measure of correlation interactions and their impact on the magnetic properties of the double perovskites. One can see that $I_{\rm OEP}^{\tau}$ is reduced by about 10-20% in comparison with $I_{\rm HF}^{\tau}$, which indicates the importance of correlation interactions.

Finally, it is instructive to consider the effect of the static screening alone. The

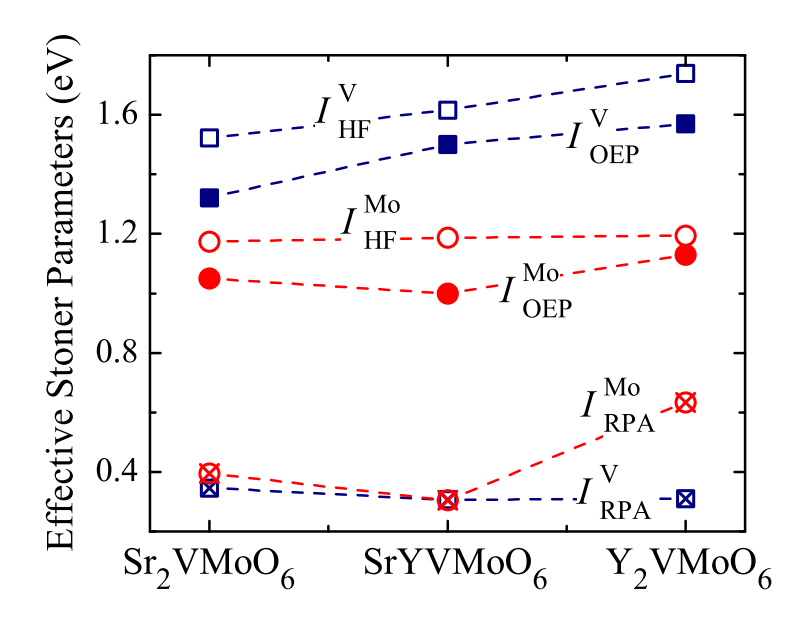


Figure 7. Effective Stoner parameters for $Sr_{2-x}Y_xVMoO_6$ as derived in the optimized effective potential (OEP) method for the ferrimagnetic state, in the Hartree-Fock (HF) approximation, and using only static values of Coulomb and exchange interactions in the random phase approximation (RPA).

corresponding on-site interaction parameters in RPA are given by

$$\hat{U}_{\text{RPA}} = \frac{1}{\Omega_{\text{BZ}}} \int d\mathbf{q} \left[1 - \hat{U}\hat{P}(0, \mathbf{q}) \right]^{-1} \hat{U},$$

which yields the Stoner parameter $I_{\text{RPA}}^{\tau} = (\mathcal{U}_{\text{RPA}}^{\tau} + 2\mathcal{J}_{\text{RPA}}^{\tau})/3$. Such a picture can be regarded as the static limit of the GW approximation [27, 28], where the frequency-dependent screened Coulomb interaction $\hat{U}_{\text{RPA}}(i\omega)$ is replaced by its static counterpart $\hat{U}_{\text{RPA}} \equiv \hat{U}_{\text{RPA}}(0)$ [29]. Typically, it is sufficient to consider only site-diagonal contributions to \hat{U}_{RPA} , because if \hat{U} is site-diagonal, the off-diagonal contributions to \hat{U}_{RPA} are expected to be small [30]. These results are also shown in Fig. 7. One can clearly see that the parameters I_{RPA}^{τ} are overscreened and strongly underestimated in comparison with I_{OEP}^{τ} . This indicates the importance of dynamical screening effects in the construction of the optimized effective potential.

3.3. Total energy and stability of the ferrimagnetic state

The behavior of the total energy and of its partial contributions is explained in Fig. 8. For all considered compounds, except Sr_2VMoO_6 , the ferrimagnetic configuration has lower energy. The tendencies towards ferrimagnetism increase with the band-filling. The main factor stabilizing the ferrimagnetic state is the gain of the kinetic energy. The main factor destabilizing it is the loss of the exchange energy.

In order to investigate the local stability of the ferrimagnetic phase, we calculate the spin stiffness D, which is related to the second derivative of the total energy with

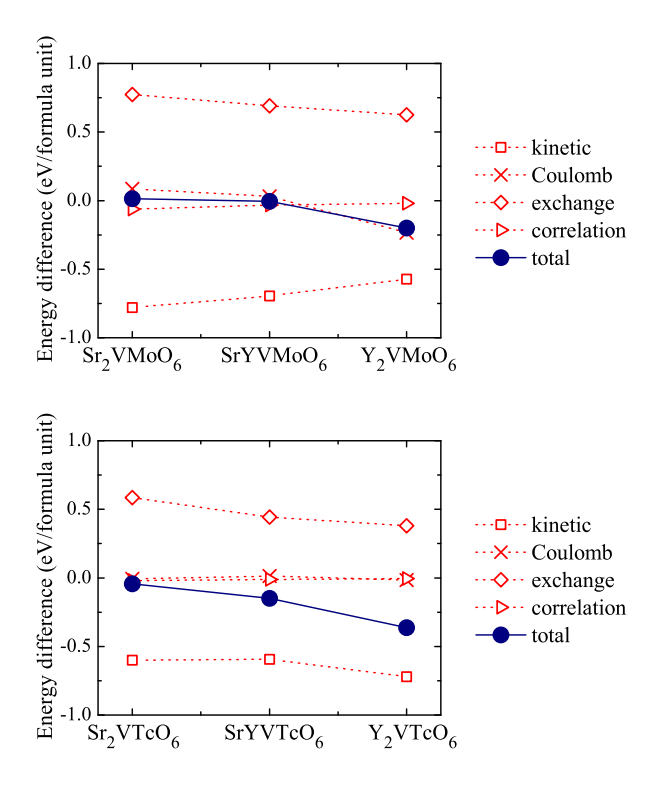


Figure 8. Total energy difference between ferrimagnetic and ferromagnetic states and partial contributions to this energy difference, calculated for $Sr_{2-x}Y_xVMoO_6$ (top) and $Sr_{2-x}Y_xVTcO_6$ (bottom).

respect to the spin-spiral vector \mathbf{q} in the ferrimagnetic state:

$$E(\mathbf{q}) \approx E(\mathbf{q}_0) + D(\mathbf{q} - \mathbf{q}_0)^2,$$

where $\mathbf{q}_0 = (\pi/a, \pi/a, \pi/a)$ and a is the cubic lattice parameter. More specifically, the numerical calculations of $E(\mathbf{q})$, were performed by employing the generalized Bloch theorem [31] and the so-called local-force theorem for the infinitesimal spin rotations. The latter states that the total energy change for the small rotations can be replaced by the change of the one-electron energies, obtained from the Kohn-Sham equations (2) for the rigid spin rotations of the effective potential $\hat{v}_{\text{eff}}^{\sigma}$ [32]. The theorem is rather general and can be proven by considering the rotational invariance of the exchange-correlation functions [8]. Thus, the range of the applicability of this theorem is not limited by the local-spin-density approximation, for which it was originally proven, but can be also extended to the OEP approach [8], provided that the effective potential $\hat{v}_{\text{eff}}^{\sigma}$ is uniquely defined. Particularly, since the choice of $\hat{v}_{\text{eff}}^{\sigma}$ is not unique in the case of insulating Y₂VTcO₆, this strategy cannot be directly applied to this system.

The behavior of D in the OEP model is explained in Fig. 9. Particularly, D is negative in the case of Sr_2VMoO_6 , Sr_2VTcO_6 , and $SrYVMoO_6$. Thus, the ferrimagnetic state in these compounds is unstable with respect to the incommensurate spin-spiral state. Since FM state has lower energy in the case of Sr_2VMoO_6 (Fig. 8), the spin-spiral instability of the ferrimagnetic state may be finally resolved in the favor of the collinear

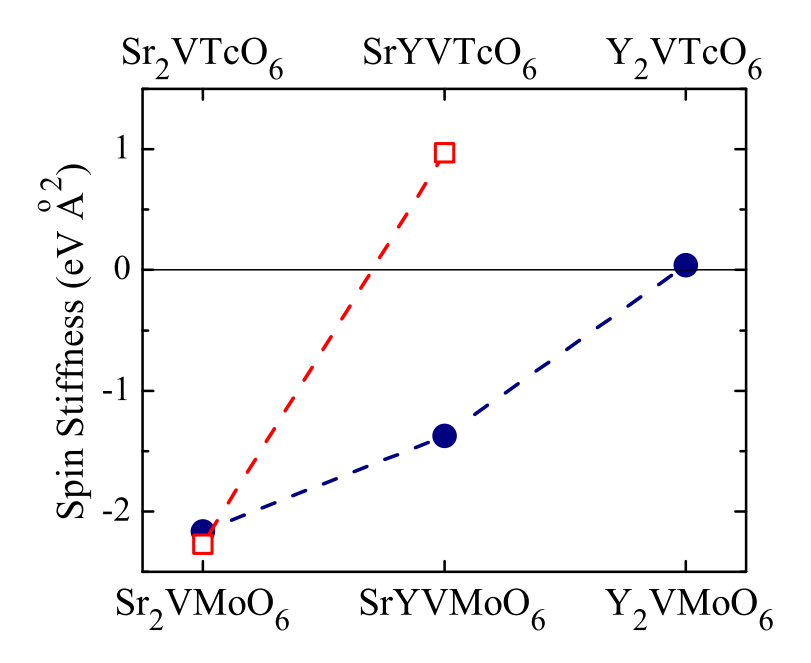


Figure 9. Spin stiffness in the ferrimagnetic state calculated using optimized effective potentials for $Sr_{2-x}Y_xVMoO_6$ (filled circles) $Sr_{2-x}Y_xVTcO_6$ (empty squares).

FM arrangement, to make it the true magnetic ground state of Sr₂VMoO₆. However, in Sr₂VTcO₆ and SrYVTcO₆ already ferrimagnetic state has lower energy. Moreover, this ferrimagnetic state itself appears to be unstable with respect to the noncollinear spin-spiral alignment. Thus, the ground state in this case will be neither ferro- nor ferrimagnetic.

4. Summary and Conclusions

In summary, using first-principles electronic structure calculations, we have constructed the effective low-energy model for the t_{2g} -states of double perovskites $\mathrm{Sr}_{2-x}\mathrm{Y}_x\mathrm{VMoO}_6$ and $\mathrm{Sr}_{2-x}\mathrm{Y}_x\mathrm{VTcO}_6$. Then, the ground-state properties of the obtained model have been investigated on the basis of the optimized effective potential method, by treating correlation interactions in the random-phase approximation. The reason for using such strategy was twofold. On the one hand, such approach allows one to improve the commonly used local-spin-density approximation for the double perovskites and incorporate the physics of electron correlations beyond the homogeneous electron gas limit. On the other hand, since OEP is formulated as the ground-state method, where all the parameters are derived rigorously by minimizing the total energy of the system, it gets rid of many ambiguities inherent to the LSDA+U method. Particularly, although $\mathrm{Sr}_{2-x}\mathrm{Y}_x\mathrm{VMoO}_6$, $\mathrm{Sr}_{2-x}\mathrm{Y}_x\mathrm{VTcO}_6$, and other isoelectronic to them compounds are frequently proposed to exhibit half-metallic ferromagnetic or antiferromagnetic properties, the situation is probably not such optimistic because of the electron correlation effects, which affect the intraatomic exchange splitting and

makes it substantially larger than in LSDA. Of course, this will revise many predictions based on the LSDA. For example, Y_2VTcO_6 , which was expected to be half-metallic antiferromagnet, appears to be insulator. The behavior of other materials is even more complicated. For the most of them (except Sr_2VMoO_6), the half-metallic ferromagnetic state is energetically less favorable than the (normal) metallic ferrimagnetic one. Nevertheless, this ferrimagnetic state appears to be also unstable with respect to the spin-spiral alignment. Thus, the true magnetic ground state of these double perovskites will be the spin spiral or some more complicated non-collinear magnetic structure.

Finally, we have argued that the effective potential (and therefore the one-electron band structure) for the half-metallic and insulating ferro- or antiferromagnetic state is not uniquely defined. Generally, there is a bunch of parameters, which yield the same total energy, occupation numbers and spin magnetic moments at the transition-metal sites.

Acknowledgments

I wish to thank the support from the Federal Agency for Science and Innovations, grant No. 02.740.11.0217, during my stay at the Ural State Technical University (Ekaterinburg, Russia).

References

- [1] Serrate D, De Teresa J M and Ibarra M R 2007 J. Phys.: Condens. Matter 19 023201
- [2] Kobayashi K-I, Kimura T, Sawada H, Terakura K and Tokura Y 1998 Nature 395 677
- [3] Solovyev I V 2002 Phys. Rev. B **65** 144446
- [4] van Leuken H and de Groot R A 1995 Phys. Rev. Lett. 74 1171
- [5] Pickett W E 1998 Phys. Rev. B **57** 10613
- [6] Anisimov V I, Zaanen J and Andersen O K 1991 Phys. Rev. B 44 943
- [7] Solovyev I V, Dederichs P H and Anisimov V I 1994 Phys. Rev. B 50 16861
- [8] Solovyev I V and Terakura K 1998 Phys. Rev. B 58 15496
- [9] Kohn W and Sham L J 1965 Phys. Rev. 140 A1133
- [10] Talman J D and Shadwick W F 1976 Phys. Rev. A 14 36
- [11] Kotani T and Akai H 1996 Phys. Rev. B **54** 16502
- [12] Kotani T 1998 J. Phys.: Condens. Matter 10 9241
- [13] Engel E and Schmid R N 2009 Phys. Rev. Lett. 103 036404
- [14] Gotoh H, Takeda Y, Asano H, Zhong J, Rajanikanth A and Hono K 2009 Applied Physics Express 2 013001
- [15] Park M S and Min B I 2005 Phys. Rev. B **71** 052405
- [16] Wang Y K, Lee P H and Guo G Y 2009 Phys. Rev. B 80 224418
- [17] Park J H, Kwon S K and Min B I 2002 Phys. Rev. B 65 174401
- [18] Uehara M, Yamada M and Kimishima Y 2004 Solid State Commun. 129 385
- [19] Song W, Wang J, Meng J and Wu Z 2010 J. Comp. Chem. 31 1795
- [20] Solovyev I V 2008 J. Phys.: Condens. Matter **20** 293201
- [21] Kanamori J 1963 Prog. Theor. Phys. **30** 275
- [22] Pines D 1999 Elementary Excitations in Solids (Oxford: Westview Press)
- [23] von Barth U and Hedin L 1972 J. Phys. C 5 1629
- [24] Aryasetiawan F, Miyake T and Terakura K 2002 Phys. Rev. Lett. 88 166401

- [25] Mazin I I 1999 Phys. Rev. Lett. 83 1427
- [26] Gunnarsson O 1976 J. Phys. F **6** 587
- [27] Hedin L 1965 Phys. Rev. 139 A796
- [28] Aryasetiawan F and Gunnarsson O 1998 Rep. Prog. Phys. 61 237
- [29] Aryasetiawan F, Imada M, Georges A, Kotliar G, Biermann S and Lichtenstein A I 2004 *Phys. Rev.* B **70** 195104
- [30] Solovyev I V 2006 Phys. Rev. B **73** 155117
- [31] Sandratskii L M 1998 Adv. Phys. 47 81
- [32] Bruno P 2003 Phys. Rev. Lett. 90 087205